# Large Eddy Simulation of the flow over periodic hills

C. P. Mellen* J. Fröhlich* W. Rodi*

**Abstract**

Results are reported from Large Eddy Simulations of the flow over periodic hills. The geometry used is based on a previous experiment but the authors have departed from the original configuration in a number of ways. The result is a computationally affordable test case displaying separation, strong recirculation and natural reattachment. The computations reported here have concentrated on two key areas. The first is the evaluation of existing SGS models. Stability issues, sensitivity to grid filter sizing and suitability for use in recirculating flow are assessed. Secondly, the usefulness of near-wall models devised for attached flow regimes is assessed by comparisons with a particular scaling for recirculating flows.

**Key words:** Large Eddy Simulation, separated flow, wall modelling, subgrid-scale modelling.

**AMS subject classifications:** 58D30, 76F65.

## 1 Introduction

The Institute for Hydromechanics is one of the partners currently involved in the LESFOIL project funded by the European Community. LESFOIL is intended to assess the feasability of using Large Eddy Simulations to compute the flow over high $Re$ airfoils at large angles of attack. The airfoil selected for investigation is the Aerospatiale A-airfoil. The flow conditions have been set to be $Re_c = 2 \times 10^6$ and $\alpha = 13.3°$. For these conditions the experimental data indicates the existence of separated turbulent flow over the last 15 % of the airfoil's suction surface. The capture and modelling of this separation is one of the challenges faced by the LESFOIL partners. The computation of this high $Re$ flow has emphasised the importance of suitable near-wall and subgrid-scale models. Naturally, the need has arisen a test case which can be easily computed and which can be used to evaluate these models under conditions of separated flow. As well as being easily computable, it is desired that the test case display strong recirculation and preferrably, natural reattachment. Additionally, its geometry should be plane in the spanwise direction. The purpose of this paper is to present such a test case and to report on some of the computations which have already been conducted on it.

The literature contains many examples of both computational and experimental investigations into separated flow with reattachment. Only a few of these flows were considered to be potential test case candidates. As an example, the flows involving 2D backward-facing steps were disregarded due to the nature of the separation being completely determined by the step geometry. Other flows, such as the asymmetric diffuser studied by Kaltenbach [4] were rendered unsuitable by the expense of the computations . A DNS of an entire turbulent separation bubble, undertaken by Na and Moin [5], is in fact available. Unfortunately, the Reynolds number of the flow was necessarily quite low, $Re_\tau = 180$, making it not particularly relevant to the airfoil situation. Other authors have investigated the flow over wavy or sinusoidal terrain or over 2D hills. Of these latter investigations of most interest to the LESFOIL partners were the experiments of Almeida *et al* [1]. These experiments had in fact been the basis of a test case examined during the 1995 ERCOFTAC/IAHR workshop held at Karlsruhe University [3]. Data is available for two different configurations : flow over a single hill and flow over periodic hills. It was felt that one or the other of these configurations would provide a test case suitable for studying SGS and near-wall modelling in the presence of separation and reattachment.

*All authors : Institute for Hydromechanics, University of Karlsruhe, Germany. <lastname>@ifh.bau-verm.uni-karlsruhe.de

16th IMACS World Congress (© 2000 IMACS)

Initial computations were subsequently performed at the IfH on what was judged to be the least demanding configuration : this was the periodic hill without sidewalls. Based on hill height and mean centreline velocity the Reynolds number for these calculations was $Re = 60000$, while the Reynolds number based on the height of the channel containing the hills was $Re = 365000$. These calculations highlighted a number of problems with the chosen test case - primarily the high computational cost of the chosen configuration and the unknown influence of the sidewalls in the experiment. As well, no reliable experimental data is available for this configuration as the results from the 1995 ERCOFTAC/IAHR workshop have cast doubt on the true periodicity of the experimental configuration. Suitable experimental data is available for the single hill geometry discussed in [1], however this configuration is computationally even more demanding than the periodic case, and the question of the influence of the sidewalls would still persist. It was therefore decided to define a new geometry, independent of experiments, which would provide an easily computed test case containing flow separation and reattachment. Although no experimental data would be available, the ability to perform comparitive studies of wall and SGS models will be instructive and useful. To provide some reference it was decided that a wall-resolving computation using the dynamic SGS model would be performed. In addition, it is now likely that workers at the University of Surrey will undertake an experimental investigation of this new test case and so provide definitive reference data.

## 2 Test Case Geometry

The new geometry, shown in Fig. 1, retains the shape of the hill defined by Almeida [2]. However, the original periodic hill geometry separated the hill crests by $L_x = 4.5h$ - where $h$ is the hill height - the new geometry has increased this distance to $L_x = 9.0h$. The original channel height $L_y$ was $6.07h$. In the new geometry this distance has been halved so that $L_y = 3.035h$. The Reynolds number for the computation has also been reduced. Based on hill height and bulk velocity in the channel the new Reynolds number has been defined to be $Re_h = 7100$ while for the channel height the bulk Reynolds number is $Re_{Ly} = 21560$. The spanwise width for the computational domain has been set to $L_z = 4.5h$.

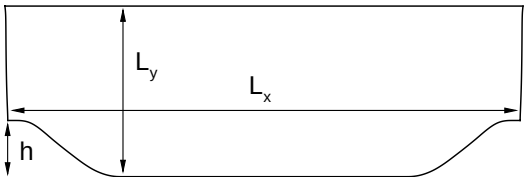


Figure 1: Test case geometry

The increase in distance between hill crests is intended to reduce concerns about possible high levels of flowfield correlation between the streamwise periodic boundaries. The added distance also introduces variability into the reattachment point of the separated shear layer. In the original experimental configuration this location was dictated by the presence of the windward face of the second hill. Reattachment now occurs naturally and is hence influenced by wall modelling, SGS modelling and grid arrangement. The decrease in channel height from $6.07h$ to $3.035h$ allows a higher aspect ratio channel to be more easily computed. The new geometry specifies an aspect ratio of 1.5 and, importantly, is defined so as to be without sidewalls. Periodic conditions are applied in the spanwise direction. Optimally, an even larger aspect ratio would be specified, thus reducing the spanwise correlation of the flow. Constraints are imposed however by the available computational resources. Nonetheless, since all tests performed by the project partners are conducted with the same value of $L_z$ reliable studies of SGS and wall modelling can be undertaken.

## 3 Computations

To date six computations have been completed, encompassing four grids and two SGS models as summarised in Table. 1. These computations have been performed using the Finite Volume code LESOCC [7] parallelised by domain decomposition and explicit message passing. It employs a collocated discretisation and curvilinear coordinates with second order central schemes in space and a Runge-Kutta time stepping together with the SIMPLE procedure. Other LESFOIL partners have undertaken additional computations, though they will not be reported here.

Computations C1,C2,C4 & C5 have assessed the impact of different SGS models and also the effect of grid refinement. C6 is the wall-resolving reference computation. This computation was undertaken on 96 nodes of an IBM RS/6000 SP and required approximately 60000 hours of processor time for 205000 timesteps at $\Delta t \approx 3 \times 10^{-4} L_x/U_b$

| Comp. | SGS model | Wall model | Grid | $L_z$ | $t_{int}$ | $x_{sep}/h$ | $x_{reat}/h$ |
|---|---|---|---|---|---|---|---|
| C1 | Smag | W-W | $118 \times 66 \times 96$ | $4.5h$ | 120 | 0.45 | 3.60 |
| C2 | Dyn | W-W | $118 \times 66 \times 96$ | $4.5h$ | 115 | 0.50 | 3.20 |
| C3 | Dyn | W-W | $118 \times 66 \times 194$ | $9.0h$ | 25 | 0.45 | 3.25 |
| C4 | Smag | W-W | $182 \times 66 \times 96$ | $4.5h$ | 100 | 0.32 | 4.70 |
| C5 | Dyn | W-W | $182 \times 66 \times 96$ | $4.5h$ | 100 | 0.30 | 4.23 |
| C6 | Dyn | no-slip | $202 \times 130 \times 196$ | $4.5h$ | 55 | 0.20 | 4.56 |

Table 1: Overview of computations performed ($t_{int}$ = integration time in terms of flow through times)

. Computations C1-C5 required 8-10000 hours of processor time using 48 nodes and 140000 timesteps at $\Delta t \approx 8 \times 10^{-4} L_x/U_b$. C3 was to assess the relationsip between the spanwise correlation and the width of the domain. In the $x$-$y$ plane this grid is identical to that used in C1 & C2. For reasons of economy this computation was not progressed to a statistically converged state. All computations except C6 used the Werner-Wengle model to treat the near-wall region of the flow.

A planar view of the $118 \times 66 \times 96$ and the $182 \times 66 \times 96$ grids are given in Fig. 2. In the near wall region the grid used in C1 - C3 is nearly uniformly spaced whereas the grid for C4 & C5 has been refined in the streamwise direction in the area around the hill crest so as to better resolve the flow around the separation point. Additionally, this grid is slightly stretched normal to the lower wall. The wall resolving grid used in C6 had $y^+ < 1$ for 95% of the grid points adjacent to the lower wall. As well, this grid was designed so that this wall region would be resolved by 8-10 grid points with $y^+ \leq 10$. All grids are uniformly spaced in the spanwise direction. In the figures which follow the $118 \times 66 \times 96$ mesh is referred to as Grid 1, while the $182 \times 66 \times 96$ mesh is denoted Grid 2.

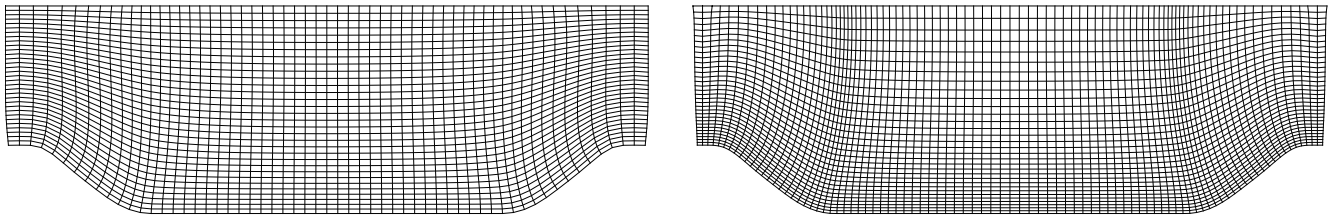

Figure 2: Grid 1 and Grid 2. Note : every 2nd grid line omitted for display purposes

# 4 Description of Flow

All computations indicate similar flow features. Typical mean streamlines are shown in Fig. 3. After traversing the crest of the leading hill, the flow separates at $x/h \sim 0.2-0.4$. Downstream of separation a strong separated shear layer is evident and a large region of recirculating fluid may be found in the lee of the hill. The flow generally reattaches at $x/h \sim$ 3.5-4.5. The exact value varies with SGS model and grid. On the finer grids a small recirculation region forms on the windward side of the following hill. Such a recirulation was also found by Almeida [1] in his single hill experiment.

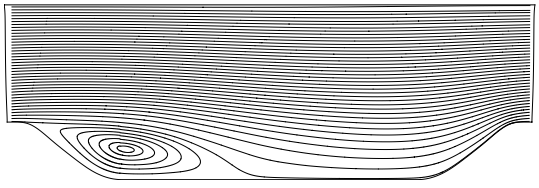

Figure 3: Typical mean streamlines

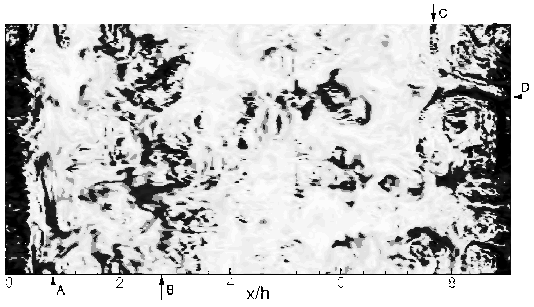


Figure 4: Near-wall vorticity

Fig. 4 shows a snapshot of the absolute value of vorticity for a plane close to the lower wall. This figure is marked with four arrows, labelled A,B,C, & D. Inside the main recirculation region small-scale spanwise-oriented turbulent structures can be seen at 'A'. 'B' indicates that once past $x/h \sim 2.0$ the orientation of this structure changes to a primarily streamwise direction. It is interesting that this change coincides approximately with the location of the maximum near-wall backflow shear stress. A further near-wall small-scale spanwise structure, marked by 'C', occurs at about $x/h = 7.5$. This is the region around the potential secondary recirculation mentioned previously. 'D' points to evidence of Görtler vortices forming on the windward face of the following hill. These vortices stretch to near the hill crest and are easily discernible when the flowfield further from the wall is examined.

Away from the lower wall just outside the recirculation region the structure is oriented predominately in the spanwise direction. This structure is of quite large scale and may at any one time be coherent over 30-40% of the domain width and 20% of the domain length. This last observation raises the question of the spanwise velocity correlations for the flow. Ideally one would like the correlations to vanish as $d_z/L_z \rightarrow 0.5$. Fig. 5 indicates the spanwise correlation of the $u$ component of velocity at two different locations in the domain, taken from C5. The correlation taken at $(x/h, y/h) = (3.57, 1.04)$ is located very close to the detached shear layer. It can be seen that at $d_z/L_z = 0.5$ the correlation level is in fact signficant. Though not shown, the results from C3 indicate that doubling the width of the domain produces close to the desired correlation levels. However, a domain width of $L_z = 9.0h$ leads to prohibitive computational costs. We are of the opinion that a non-zero spanwise correlation does not adversely impact on the comparisons we wish to undertake.

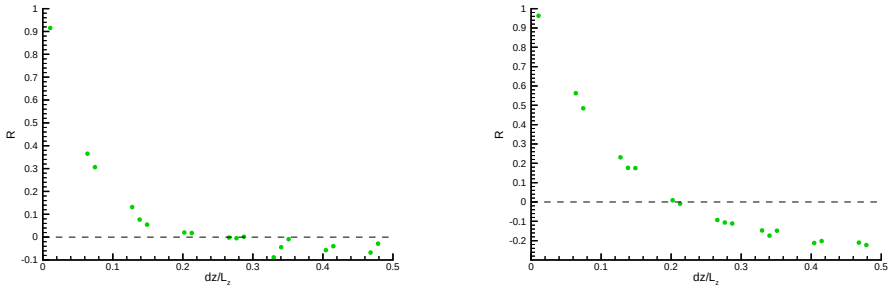


Figure 5: Spanwise $u$ correlation, left : $(x/h, y/h) = (1.77, 0.18)$, right : $(x/h, y/h) = (3.57, 1.04)$

## 5 Discussion of Results

The results obtained exhibit sensitivity to the SGS model and the grid employed. Fig. 6 shows the shear stress at the lower wall (<> indicates averaging in $z$ and time). It appears that the point of flow separation is little influenced by the choice of the subgrid model, but is dependant on the amount of grid refinement around the crest of the hill. Grid 1 is simply too coarse in this area. In contrast, the reattachment location is affected by both the model employed and the grid used. Refining the grid increases the separation length while employing the dynamic SGS model instead of the Smagorinsky SGS model causes the separation length to become shorter. These trends are summarised in the last two columns of Table 1.

Generally, all $\tau_w$ curves are similar, though in the region between $x/h \sim 0.4$ and $x/h \sim 2.0$ the computation with the wall-resolving grid and dynamic SGS model combination shows details which are only hinted at by the other simulations. Fig. 7 reports the distance from the wall to the first computational point for the computations with the dynamic SGS model. For the majority of the flow the computations on the wall-function grids have these points located at $y^+ \leq 6$, i.e., in the viscosity dominated near-wall region. When the first point is so close to the wall the Werner-Wengle wall model employs what is effectively a no-slip condition. Essentially, the choice of wall model has had little effect on the outcome of these computations. It can also be seen that over the majority of the lower wall, the wall-resolving grid successfully placed the first computational point below $y^+ = 1$.

Figures 8-10 show mean profiles along the line $x/h = 2.0$ for selected flow variables while Figure 11 compares the ratio $< \nu_t > /\nu$ at the same location. Variation with grid and SGS model can be observed. Especially noticeable is that the dynamic SGS model consistently predicts levels of turbulent viscosity signficantly larger than those given by the Smagorinsky model. The deviations in the other quantities are attributable to this. Similar observations can be made at other locations within the flow domain. The differences between the $\nu_t$ levels predicted by the two SGS models are

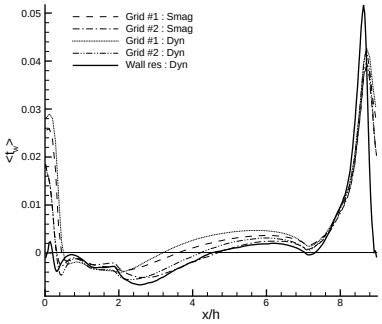


Figure 6: $\tau_w$ at lower wall

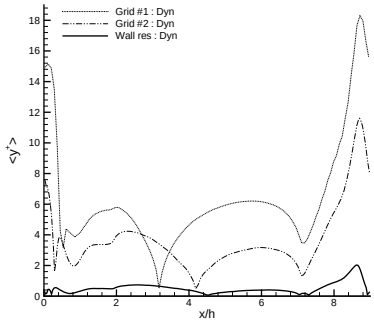


Figure 7: $y_1^+$ at lower wall

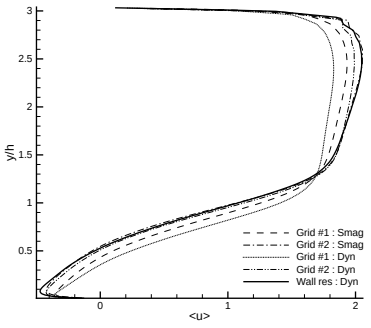


Figure 8: $< u >$ at $x/h = 2.0$

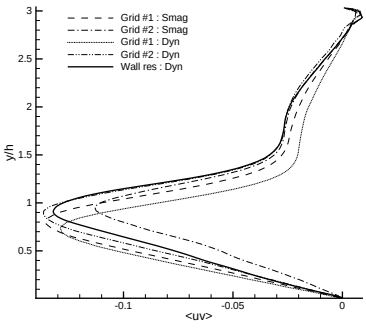


Figure 9: $< uv >$ at $x/h = 2.0$

largest just after separation, at $x/h \sim 0.5$. Here, in the separated shear layer, the ratio $(< \nu_{t.dyn} > / < \nu_{t.Smag} >)_{max}$ increases to approximately 7.5. Further down the channel it drops back once more to around 3-4. Some of this can presumably be attributed to the usual uncertainty inherent in the specification of the Smagorinsky constant ($C_s = 0.1$ was employed). However, it does seem as if the dynamic SGS model is displaying sensitivity to poor grid resolution in the more energetic regions of the flow. This behaviour is still under investigation.

# 6 New near-wall model for separated flow

One of the reasons for studying the hill flow is to facilitate the development of new near-wall laws intended for use in recirculating flow. Figs. 12 and 13 show velocity profiles taken from within the recirulation zone of the wall-resolving computation. In Fig. 12 these profiles have been normalised using the standard log-law assumption while in Fig. 13 a parameterisation specifically intended for use with recirculating flow [6] has been applied. It assumes that the velocity profile inside a region of recirculation may be described by :

$$U^* = \frac{1}{\kappa}(y^* - ln(y^*) - 1) \tag{1}$$

Here $y^* = y/y_N$, $U^* = (U + |U_N|)/U_\tau$, where $|U_N|$ is the magnitude of the maximum backflow velocity, $U =< u >$ and $y_N$ is the distance from the wall to the point of maximum backflow. Fig. 12 illustrates the unsuitability of the log-law scaling. Furthermore the accuracy of the no-slip assumption cannot be relied upon if $y_1^+$ is larger than $\sim 1$. When the new 'backflow' scaling is employed the profiles collapse quite satisfactorily, as shown in Fig. 13. The sucess of this and other *a priori* tests have prompted the development of a new LES near-wall model based on this latter scaling. Results will be reported in future articles.

# 7 Conclusions

A computationally affordable test configuration for the LES of recirculating flows has been developed and computations, including a reference wall-resolving computation, have been reported for a new test case featuring recirculating

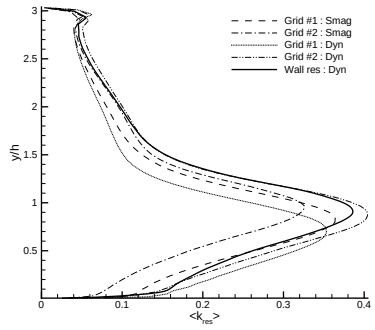


Figure 10: $< k_{res} >$ at $x/h = 2.0$

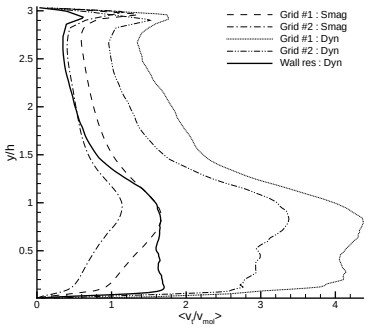


Figure 11: $< \nu_t > /\nu$ at $x/h = 2.0$

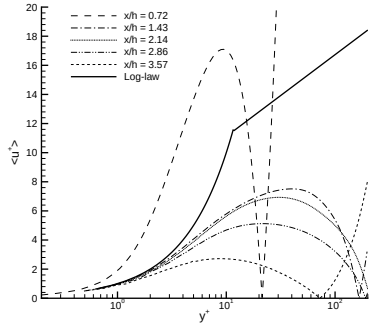


Figure 12: Log-law scaling

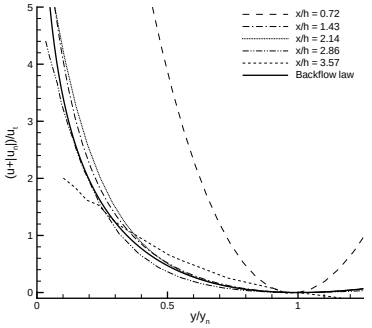


Figure 13: 'Backflow' scaling

flow. The sensitivity of the results to grid and SGS model variations have been assessed and some interesting behaviour of the dynamic SGS model has been observed. As well, *a priori* tests of a new scaling law intended for use in recirculating flow have been sucessfully undertaken. Computations using the backflow wall model for a *posteriori* test are currently underway.

**Acknowledgements :** The authors acknowledge funding through the LESFOIL project and the computation time provided by the University of Karlsruhe.

# References

[1] G.P. Almeida, D.F.G Durao and M.V. Heitor, *Wake flows behind two dimensional model hills*, Exp. Thermal and Fluid Science., 7 (1993), pp. 87-101.

[2] G.P. Almeida, D.F.G Durao and M.V. Heitor, *ERCOFTAC "Classic Collection" database*, Exp. C18, http://vortex.mech.surrey.ac.uk.

[3] *4th ERCOFTAC/IAHR Workshop on Refined Flow Modelling*, April 3-7, 1995, University of Karlsruhe, Germany.

[4] H.J. Kaltenbach, M. Fatica, R. Mittal, T.S. Lund and P. Moin, *Study of flow in a planar asymmetric diffuser using large-eddy simulation*, Journal of FLuid Mechanics, 390 (1999), pp. 151-186.

[5] Y. Na and P. Moin, *Direct numerical simulation of turbulent boundary layers with adverse pressure gradient and separation*, Report TF-68 (1996), Thermosciences Division, Dept. Mech. Eng., Stanford University.

[6] F. Mathey, J. Fröhlich and W. Rodi, *In Preparation.*

[7] F. Mathey, J. Fröhlich and W. Rodi, *Large Eddy Simulation of the flow over a matrix of surface mounted cubes*, in Lecture Notes in Physics, 529, Springer, 1999, pp. 153-163.